Article:

Clarke, S.D., Fay, S.D., Warren, J.A. et al. (5 more authors) (2016) Predicting the role of geotechnical parameters on the output from shallow buried explosives. International Journal of Impact Engineering, 102. pp. 117-128. ISSN 0734-743X

https://doi.org/10.1016/j.ijimpeng.2016.12.006

Predicting the role of geotechnical parameters on the output from shallow buried explosives

S.D. Clarke[a,*], S.D. Fay[a,b], J.A. Warren[a,b], A. Tyas[a,b], S.E. Rigby[a], J.J. Reay[b], R. Livesey[c], I. Elgy[c]

[a] *Department of Civil & Structural Engineering, University of Sheffield, Mappin Street, Sheffield, S1 3JD, UK*
[b] *Blastech Ltd, The Sheffield Bioincubator, 40 Leavy Greave Road, Sheffeld, UK, S3 7RD*
[c] *Physical Sciences Group, DSTL Porton Down, Salisbury, SP4 0JQ, UK*

Abstract

Experiments have been conducted to quantify the effect the geotechnical conditions surrounding a buried charge have on the resulting output. From the results obtained the critical importance of moisture content in governing the magnitude of impulse delivered is highlighted. This has led to the development of a first-order predictive model for the impulse delivered from a buried charge, based on bulk density and moisture content, allowing rapid assessment of the effect of varying the geotechnical conditions.

The work utilised a half-scale impulse measurement apparatus which incorporated a deformable target plate. Impulse, peak and residual target deflections were recorded for each test. No variations the charge geometry, mass of explosive, burial depth or stand-off were considered, with the focus solely being on the effect of the geotechnical conditions on the magnitude of loading and structural response. Five different types or grades of soils were used in the work, with both cohesive and cohesionless soils represented. Novel tests with natural beds of clay soil have provided evidence for a fundamental change in loading mechanism between cohesionless and cohesive soils. The effect of air voids on the impulse generated was also investigated which showed that while strongly correlated, air voids alone is a poorer predictor of impulse than moisture content.

Keywords: Buried charges, Impulse, Geotechnics, Soil, Plate deformation, IEDs

[*]Tel.: +44 (0) 114 222 5703
Email address: `sam.clarke@sheffield.ac.uk` (S.D. Clarke)

1. Introduction

The accurate quantification of the loading and structural deformation occurring when a shallow buried charge is detonated has received considerable attention in recent times. The conducted research has equal applicability in both civilian (de-mining) and military (protection from improvised explosive devices (IEDs)) arenas. The role geotechnical conditions play in our understanding of the mechanisms of load transfer from buried mines and IEDs is critical to our ability to protect against such events. In the first instance knowledge of which measurable geotechnical parameters can indicate an increased output from a mine or IED can play an important role in route planning for military and civilian endeavours. These same data also allow validation of numerical models to allow a more accurate assessment of the blast loading produced by the detonation of shallow-buried explosives, to aid in future predictive work.

A large effort has been made to investigate the effects of soil on the output of buried charges. Many previous studies have concentrated on assessing the deformation of a target [1, 2, 3]. These deformation data are useful for protective system design and platform validation purposes, but fail to directly assess the effect the soil has on the distribution of the loading applied. Most direct load measurement studies have concentrated on quantifying the impulse imparted to a target, which is typically spatially integrated over the entire target face [4, 5, 6, 7, 8, 9, 10], and hence these studies only provide a single data point for the validation of numerical modelling approaches.

This research effort has identified that the geotechnical properties of the soil surrounding a buried charge are of key importance in determining the magnitude of the impulse generated, and the form of the structural response. Significant parameters have been shown to include in rank order; moisture content / saturation / air voids, bulk density, and particle size distribution. Burial depth is also known to have a significant role on the impulse generated with an initial increase in delivered impulse and plate deflection at shallow depths [2] giving rise to a reduction in the deflection and energy imparted [5] as the depth increases further.

Much attention has also been given to the generation of numerical modelling techniques for the prediction of loading from buried charges. This varies from simplified load curve type models [11] to fully 3D high-fidelity numerical modelling of the explosive, soil and air domains [12, 13].

With knowledge of the principal variables, control of the geotechnical conditions is still key to understanding the relationship between the impulse generated and the structural response. It has been shown previously that by carefully controlling the burial conditions in uniform soils very repeatable impulse data can be obtained (relative standard deviation = 1.22% for nominally identical tests [14]). The work reported herein expands on the previous data set providing both the absolute magnitude of the impulse generated from each test and the resulting peak and residual plate deformations to allow for the validation of numerical models. As in previous work the measured outputs were also benchmarked against tests conducted using a surrogate mine in a steel pot (Minepot) described in the Allied Engineering Publication on procedures for evaluating the protection level of armoured vehicles (AEP-55) [15]. The use of the Minepot removes any influence of the soil overburden giving near perfect confinement to the explosives, channelling the blast directly at the centre of the target plate.

The test series comprises 74 tests in total, with the results used to generate a first-order impulse predictive method as a function of moisture content and bulk density.

2. Geotechnical conditions

In the current research programme five different types or grades of soils have been tested at a range of moisture contents (w = mass of water / *dry* mass of solids) and bulk and dry densities (ρ, total mass of soil and water per unit volume, and ρ_d, dry mass of soil per unit volume). This leads to a natural variation in the air voids (A_v, ratio of volume of air to total volume) present in each of the soils as moisture content and initial dry density are varied.

Table 1: Soil types used in the current research

Soil	PSD	w (%)	ρ (Mg/m^3)
Leighton Buzzard 14/25 (LB)	Uniform (0.6-1.18 mm)	0-25	1.5-2.0
Leighton Buzzard 6/14 (2LB)	Uniform (1.18-2.8 mm)	0-25	1.6-2.0
Leighton Buzzard 25B grit (LBF)	Well graded (0.5-5.0 mm)	0-25	1.6-2.0
Sandy gravel (Stanag) [15]	Well graded (0-20 mm)	0-14	1.9-2.2
Brown laminated silty clay	66% $<$ 0.002 mm	~27	1.93

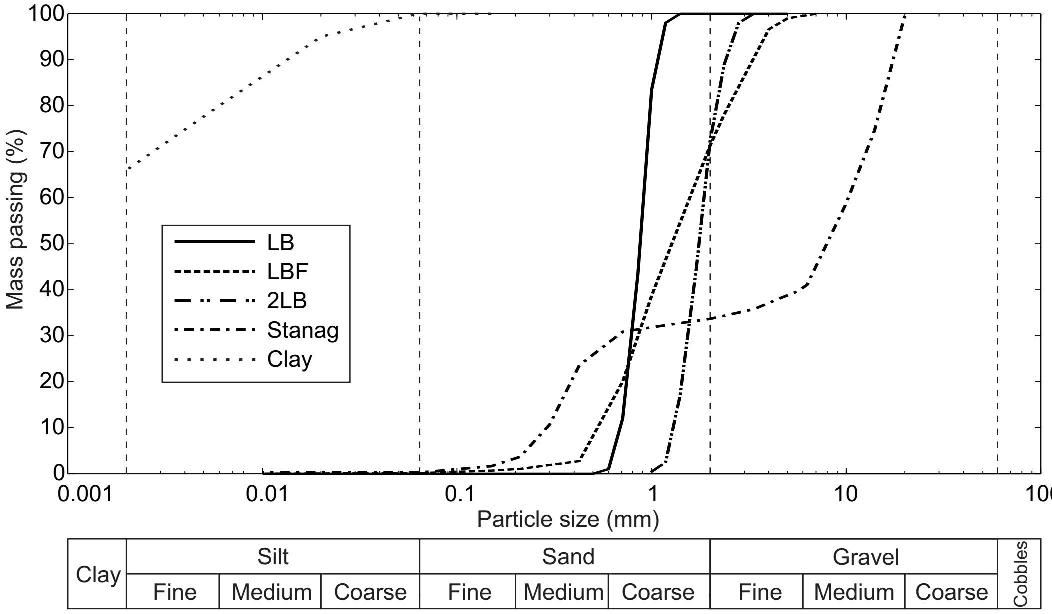

Figure 1: Particle size distributions for the soils utilised

The soil types tested are given in Table 1 with information on the particle size distribution for each soil type being shown in Fig. 1. Here, the results of a sieve analysis are plotted, with ‘mass passing’ referring to the percentage mass passing through each sieve size. Uniform soils have a small range of particle sizes and hence plot as steep lines in Fig. 1, e.g. Leighton Buzzard 14/25 (LB) and 6/14 (2LB) sands. Well graded soils have a large range of particle sizes and plot as shallow lines e.g. ‘Stanag’. The ’Stanag’ soil is similar to the sandy gravel recommended for use in buried charge tests given in AEP-55 [15], which falls within the basic parameters prescribed for NATO standardisation agreement, STANAG 4569 [16]. Three test series were conducted, series a, b and c, where the bulk density, dry density, and air void ratio were kept constant respectively. Further details on the soils tested and geotechnical preparation of the soils can be found in Ref. [14]. The target geotechnical conditions are given in Table 2. The achieved conditions are shown graphically in Fig. 2 as bulk density plotted against moisture content. This figure clearly shows that the Stanag soil has a much higher dry density (1.93 Mg/m^3) due to a lower natural porosity as the soil is well graded. This naturally leads to a high saturated bulk density (2.2 Mg/m^3) at a comparatively low moisture content. Both the LB and Clay soils achieve higher moisture contents at lower bulk densities due to the soils’ higher porosity.

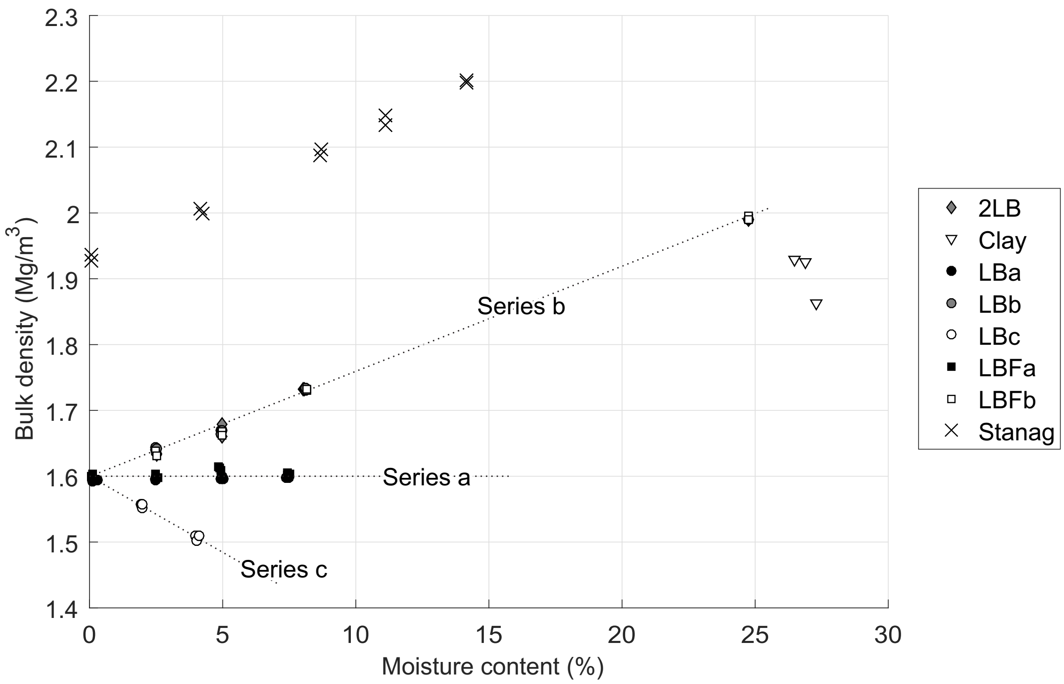

Figure 2: Moisture contents and bulk densities achieved in the testing. The dashed line series indicators are only valid for the Leighton Buzzard soils

3. Experimental setup

3.1. Test frame

The experimental work was conducted by Blastech Ltd at the University of Sheffield Blast & Impact laboratory, Buxton, UK as part of a research project funded by the UK Defence Science and Technology Laboratory (Dstl). The large test frame fabricated is shown in Fig. 3a. The deformable target plate is made from a 12.5 mm thick, 675 mm square mild steel sheet which has been modelled previously using the Johnson-Cook material model parameters given in [17]. The target plate was attached to a 675 mm square stiff interface plate, fabricated from 100 mm thick mild steel, with a 500 mm diameter circular free span for the target plate. As contact between the target plate and the internal profile of the interface plate was inevitable, the exact dimensions of the plate are given in Fig. 3b & c. The interface plate was in turn connected to a 3 m long, 500 mm diameter steel circular hollow section. The resulting system had an overall reaction mass of 1574 kg. The entire assembly was allowed to translate freely in the vertical direction after picking up load from the detonation of a buried explosive charge, with up to approx. 800 mm of vertical travel allowed. The target plates were attached to the interface

Table 2: Test plan and target geotechnical conditions

Test nos.	Soil type	Series	w (%)	ρ (Mg/m^3)	ρ_d (Mg/m^3)	A_v (%)
1–3	LB	a, b, c	0.100	1.600	1.598	39.5
4–6	LB	a	2.500	1.600	1.561	37.2
7–9	LB	a	5.000	1.600	1.524	34.9
10–12	LB	a	7.500	1.600	1.488	32.7
13–15	LB	b	2.500	1.640	1.600	35.6
16–18	LB	b	5.000	1.680	1.600	31.6
19–21	LB	b	8.100	1.730	1.600	26.7
22–24	LB	b	24.77	1.996	1.600	0.00
25–27	LB	c	2.000	1.553	1.523	39.5
28–30	LB	c	4.000	1.508	1.450	39.5
31–33	LBF	a, b	0.100	1.600	1.598	39.5
34–36	LBF	a	2.500	1.600	1.561	37.2
37–39	LBF	a	5.000	1.600	1.524	34.9
40–42	LBF	a	7.500	1.600	1.488	32.7
43–44	LBF	b	2.500	1.640	1.600	35.6
45–46	LBF	b	5.000	1.680	1.600	31.6
47–48	LBF	b	8.100	1.730	1.600	26.7
49–50	LBF	b	24.77	1.996	1.600	0.00
51–52	2LB	b	2.500	1.640	1.600	35.6
53–54	2LB	b	5.000	1.680	1.600	31.6
55–56	2LB	b	8.100	1.730	1.600	26.7
57–58	2LB	b	24.77	1.996	1.600	0.00
59–60	Stanag	b	0.100	1.929	1.927	27.1
61–62	Stanag	b	4.200	2.008	1.927	19.2
63–64	Stanag	b	8.700	2.095	1.927	10.5
65–66	Stanag	b	11.10	2.141	1.927	5.89
67–68	Stanag	b	14.15	2.200	1.927	0.00
69–71	Clay	-	27.00	1.961	1.544	0.00
72–74	Minepot	-	-	-	-	-

plate using 4 timber pegs designed to resist minimal loading, thus simplifying the boundary conditions of the plate to nominally unrestrained, with the target plate simply bearing directly onto the inner profile of the interface plate. The detached target plate was free to fall into the soil container once the event was over reducing any further deformation from the landing. Peak and residual deflections of the deformable target plate were measured post test (§3.4).

3.2. *Test configuration*

The present work used a half-geometry scale version of STANAG threat level M2 as given in AEP-55 [15], with the exception of the use of PE4 for all tests as recommended in the UK MoD Technical Authority Instructions [18]. The size of the soil container has also been scaled down to emulate the boundary conditions stipulated in AEP-55 with the exception of the boundary being cylindrical rather than rectangular. Due to the physically smaller charges being used (1/2 scale by geometry, 1/8 scale by mass and energy [19]), the Minepot was also scaled down to half scale. In each test a 625 gram charge of PE4 was buried at 50 mm, measured from the soil surface to the top of the casing. The charge was shaped into a 3:1 cylinder. The stand-off

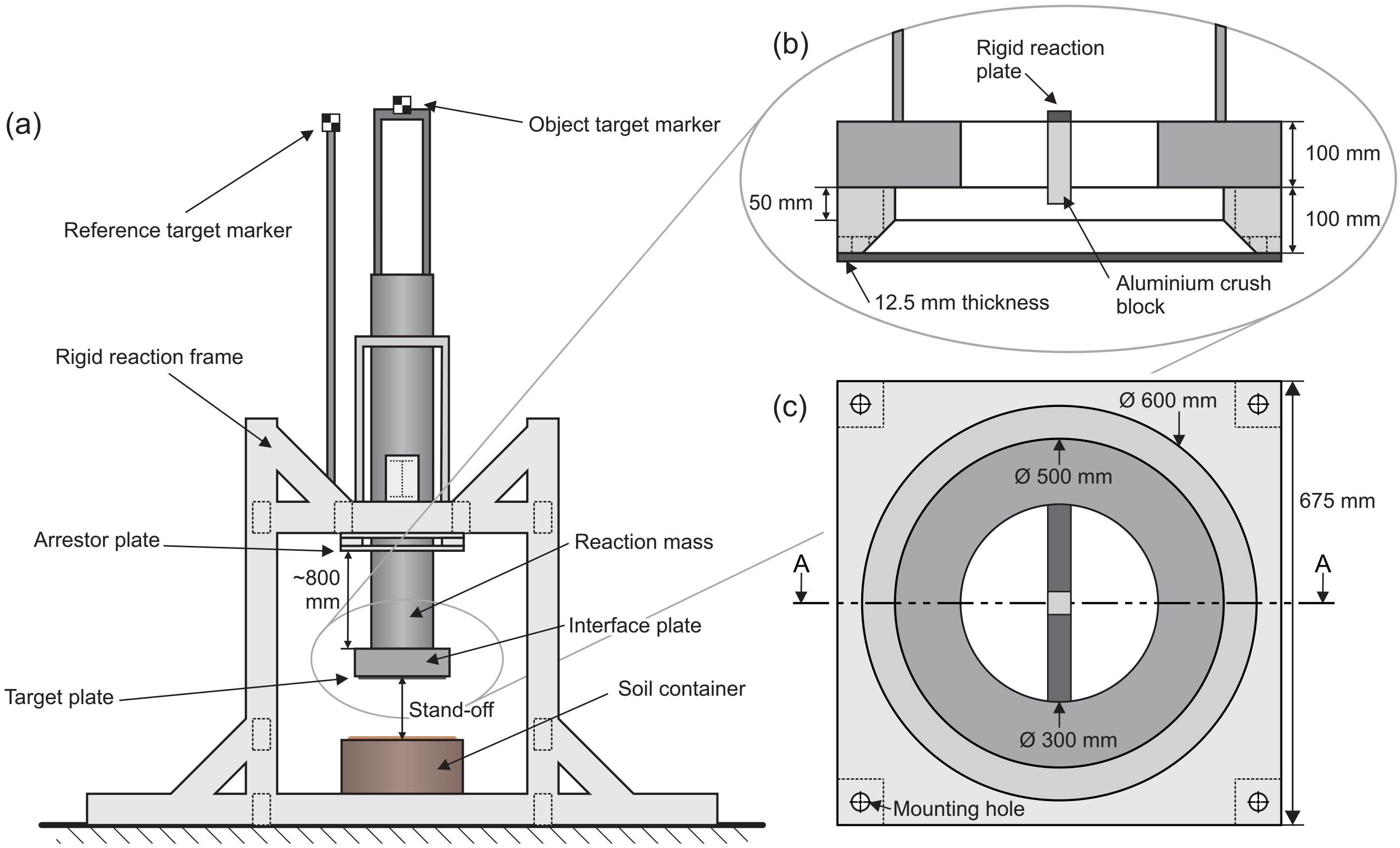

Figure 3: (a) Free-flying mass impulse capture apparatus, (b) Section through A-A showing the internal construction of the interface plate, (c) View from underneath the interface plate (with the target plate removed)

between the soil/Minepot charge surface and the target plate was 137.5 mm in all tests as shown in Fig. 4, which has been reduced from the 250 mm (500 mm full-scale stand-off) specified in AEP-55.

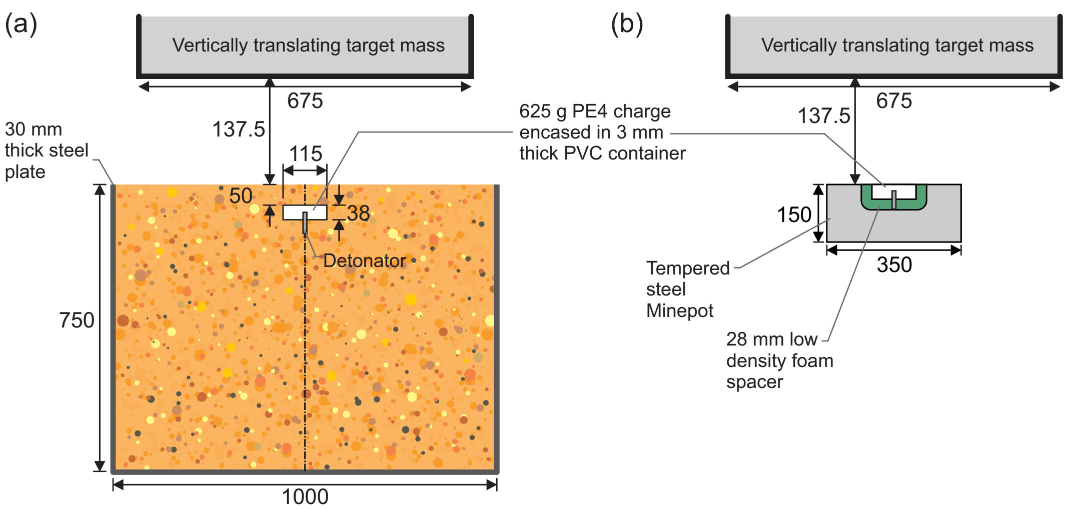

Figure 4: Details of the charge arrangement for tests utilising (a) buried charge, (b) steel Minepot

3.3. Impulse measurement

Displacement-time data of the reaction mass was measured using two target markers attached to the apparatus (Fig. 3), one to the rigid reaction frame ('reference' target marker), and the other to the rising reaction mass ('object' target marker). Both target markers are raised up on masts to delay possible obstruction by soil throw during the test. A high-speed camera (Dantec Dynamics NanoSense Mk.2, framing at 4,000 fps) was used to film the target markers. The camera was situated in protective housing on a raised structure at approximately the same height as the target markers, which made it prone to vibration from the air shock, potentially introducing an error into the marker tracking. However, since the excitation is common to both target markers, the error can be removed by subtracting the motion of the reference target marker from that of the object target marker. Using the resultant, camera-vibration corrected relative motion of the rising mass, the displacement-time history for the target can be calculated. If required (e.g. if the late-time sand throw obscures the camera), a 4th order polynomial can be fitted to the relative displacement-time curve. Whilst the displacement of the rising mass would follow a parabola under truly impulsive loading conditions, a 4th order fit was found to better represent the data, particularly in the early stages of displacement where some flexure of the frame was observed.

Fig. 5a shows the displacement-time history from Test 16, where clear oscillations are seen from image tracking of both the reference and object target markers, which can be seen to effectively cancel out when the relative displacement is taken. Here, the peak displacement of the rising mass is accurately recorded. Fig. 5b shows the displacement-time history from Test 23. Here, the displacement can only be tracked up to the point the interface plate impacts the arrestor plate, from this point onwards the polynomial provides the remaining data required to obtain the peak rise. Once the peak rise is obtained the equivalent initial velocity required to cause such a rise can then be calculated [14]. The velocity calculation assumes the velocity is applied instantaneously with the target mass subsequently free to decelerate under gravity.

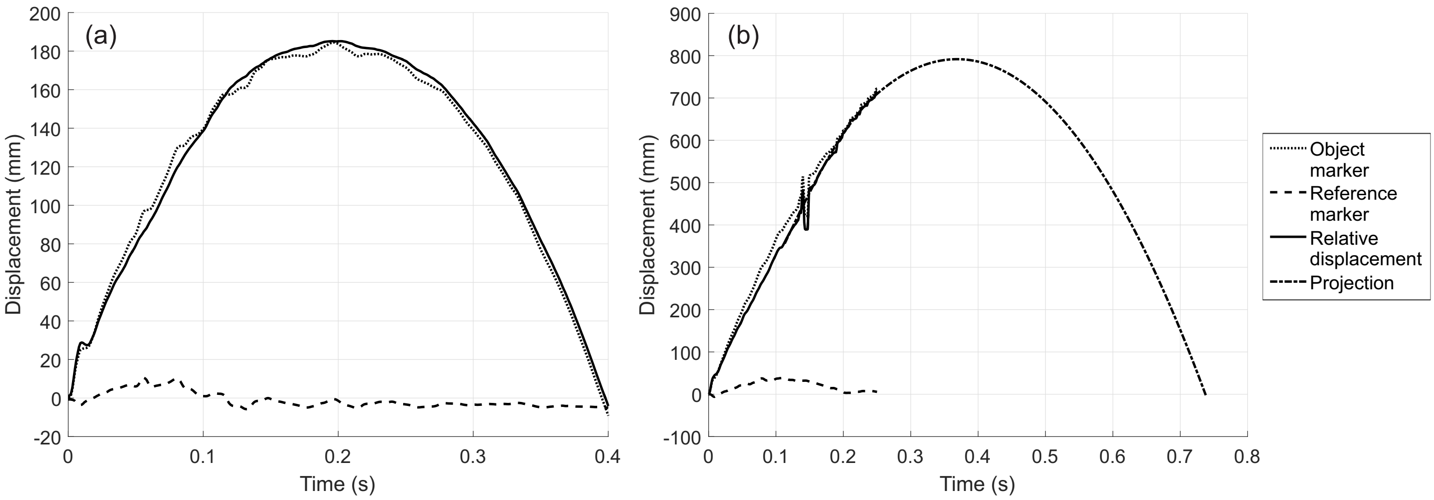

Figure 5: Example displacement-time histories (a) Test 16, LB w=4.932% ρ=1.670 I=3.00, (b) Test 23, LB w=24.77% ρ=1.990 I=6.20

3.4. Deflection measurement

For each test the peak and residual plate deflections were also recorded. The peak dynamic deformation of the target plate (relative to the interface plate) was accurately measured using a deformable aluminium honeycomb crush block, mounted on a rigid support spanning the 500 mm circular hollow section shown in Fig. 3b, c. The residual deflections were recorded post test once the plate was recovered (Fig. 6). The residual deflection was measured from the imprint of the interface plate to give readings comparable with the peak deflection. These data give an indication of the degree of focussing provided by the differing confining conditions.

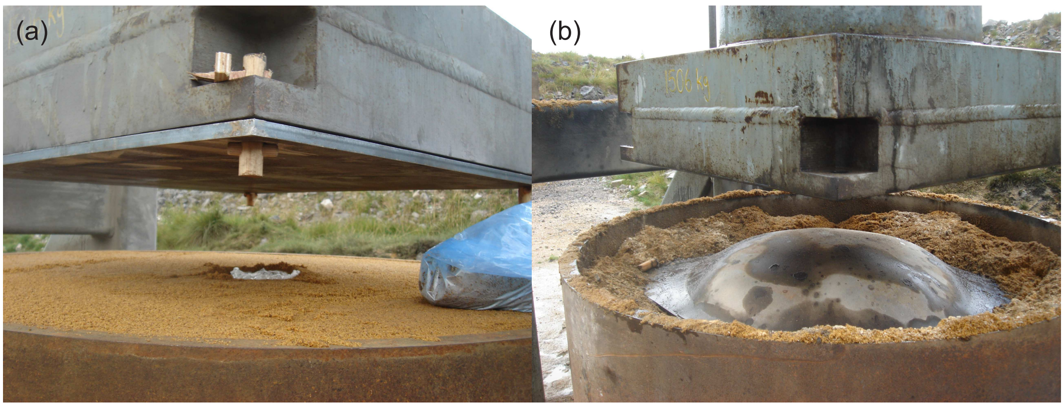

Figure 6: a) Pre-test target plate attachment detail, showing the timber dowels used, b) Post-test showing the target plate having dropped onto the remainder of the soil bed

4. Results

The results from each of the 74 tests are given in Table 3, where the achieved geotechnical conditions are reported alongside the measured impulse and deflections. The relationships between moisture content, air voids, bulk density, impulse and deflection are explored in the following subsections.

4.1. Factors affecting impulse

4.1.1. Entire test series

Fig. 7 shows the compiled data for all tests, where impulse is plotted against each of the geotechnical variables studied. At this stage, it is important to note that each sub-chart does not necessarily represent the isolated effect of each abscissa, as in certain test series an increase in moisture content also increased the bulk/dry density.

The Pearson product-moment correlation coefficient (r) for each investigated parameter is also given in Table 4. All the results in Table 4 are statistically significant ($p < 0.05$ unless indicated otherwise), with the probability of the null hypothesis being true being less than $1E-5$ in each case. Impulse and moisture content (Fig. 7a) are shown to have a very strong positive correlation ($r = 0.94$) demonstrating the high influence moisture content has on impulse. This correlation was evaluated as a first order indicator across the entire moisture content range with non-constant densities and air voids. The influence of moisture content in the low moisture content regime is systematically studied in the next section through separate consideration of series a–c tests.

Importantly, the moisture content of the confining soil has the ability to more than double the impulse being delivered to the target. When considering the two methods available in AEP-55: the use of the Minepot or fully-saturated Stanag it is clear from the results that in terms of impulse delivered the two are not equivalent. The Minepot delivers an average of 2.63 kNs compared with the 5.27 kNs from the soil.

Impulse and air voids are also shown to have a strong negative correlation ($r = -0.80$), which is in agreement with the work done by Fox [10]. However, there seems to be a limit in the ability of air voids to distinguish between different soil types when fully-saturated ($A_v = 0$).

Table 3: Achieved geotechnical conditions and experimental results, where * denotes tests where the rising mass impacted the arrestor plate and + denotes the test where late-time displacement data was obscured fully by the sand throw. For these tests, the peak displacement was extrapolated from the polynomial fit

Test no.	Soil type	w (%)	ρ (Mg/m^3)	ρ_d (Mg/m^3)	A_v (%)	Impulse (kNs)	Peak deflection (mm)	Residual deflection (mm)
1	LB	0.100	1.594	1.592	39.8	2.63	90.5	92.5
2	LB	0.100	1.593	1.591	39.8	2.73	88.5	96.0
3	LB	0.281	1.594	1.589	39.6	2.79	84.5	94.5
4	LB	2.459	1.596	1.558	37.4	2.85	86.5	93.5
5	LB	2.470	1.596	1.558	37.4	2.80	92.5	96.5
6	LB	2.480	1.595	1.556	37.4	3.14	87.5	97.0
7	LB	4.932	1.595	1.520	35.1	2.83	90.5	98.5
8	LB	4.998	1.600	1.524	34.9	2.78	95.5	100.0
9	LB	5.020	1.595	1.519	35.1	2.92	91.5	95.5
10	LB	7.388	1.598	1.488	32.9	2.83	94.5	100.0
11	LB	7.446	1.599	1.488	32.7	2.87	93.5	102.5
12	LB	7.481	1.598	1.486	32.8	3.00	89.5	98.0
13	LB	2.491	1.643	1.603	35.5	2.96	92.0	85.5
14	LB	2.491	1.641	1.601	35.6	3.03	107.0	98.0
15	LB	2.543	1.642	1.601	35.5	2.96	95.5	95.0
16	LB	4.932	1.670	1.592	32.1	3.00	113.5	103.5
17	LB	4.943	1.664	1.586	32.3	3.01	105.0	99.0
18	LB	4.998	1.670	1.591	32.0	3.08	104.0	96.5
19	LB	8.108	1.733	1.603	26.5	3.07	107.0	96.5
20	LB	8.108	1.730	1.600	26.6	3.11	102.0	98.5
21	LB	8.120	1.734	1.604	26.5	3.05	99.5	94.5
22	LB	24.77	1.990	1.595	0.31	6.30*	160.5	152.5
23	LB	24.77	1.990	1.595	0.31	6.20*	170.0	154.5
24	LB	24.77	1.990	1.595	0.31	6.13*	165.0	155.5
25	LB	1.926	1.557	1.528	39.4	2.59	96.0	94.0
26	LB	1.978	1.552	1.522	39.6	2.60	100.5	99.5
27	LB	1.999	1.558	1.527	39.3	2.92	94.0	93.0
28	LB	3.972	1.509	1.451	39.5	3.00	101.0	98.0
29	LB	4.037	1.502	1.444	39.7	2.94	98.0	95.5
30	LB	4.102	1.509	1.450	39.4	2.85	103.0	101.5
31	LBF	0.080	1.600	1.599	39.5	2.79	108.5	104.0
32	LBF	0.080	1.600	1.599	39.5	3.04	111.5	107.5
33	LBF	0.100	1.604	1.602	39.4	3.10	112.0	108.0
34	LBF	2.470	1.596	1.558	37.4	2.73	102.0	100.5
35	LBF	2.492	1.603	1.564	37.1	2.52	101.5	96.5
36	LBF	2.561	1.598	1.558	37.2	2.47	99.5	99.0
37	LBF	4.833	1.615	1.541	34.4	2.94	108.0	103.5
38	LBF	4.888	1.613	1.538	34.5	2.96	102.0	96.5
39	LBF	4.943	1.608	1.532	34.6	2.95	105.5	97.5
40	LBF	7.411	1.601	1.491	32.7	2.39	97.0	94.0
41	LBF	7.411	1.605	1.494	32.5	2.34	98.0	93.5
42	LBF	7.532	1.604	1.492	32.5	3.01	108.0	100.5
43	LBF	2.480	1.638	1.598	35.7	3.13	101.0	98.0
44	LBF	2.543	1.631	1.591	35.9	2.96	96.5	94.5
45	LBF	4.965	1.667	1.588	32.2	3.16	103.0	102.5
46	LBF	4.965	1.662	1.583	32.4	3.03	103.0	102.5
47	LBF	8.167	1.730	1.599	26.6	3.01	104.0	102.5
48	LBF	8.178	1.732	1.601	26.5	3.21	104.0	96.5
49	LBF	24.77	1.996	1.600	0.01	5.57+	153.0	146.0
50	LBF	24.77	1.990	1.595	0.31	6.16*	160.0	154.0
51	2LB	2.512	1.633	1.593	35.9	3.10	108.5	106.0
52	2LB	2.512	1.635	1.595	35.8	3.01	104.0	100.5
53	2LB	4.993	1.660	1.581	32.4	3.11	104.5	96.0
54	2LB	4.998	1.679	1.599	31.7	3.22	103.0	99.5
55	2LB	8.026	1.732	1.603	26.6	3.23	111.5	111.0
56	2LB	8.085	1.732	1.602	26.6	3.25	103.5	99.0
57	2LB	24.77	1.990	1.595	0.31	6.42*	163.0	156.0
58	2LB	24.77	1.990	1.595	0.31	6.51*	167.0	159.0
59	Stanag	0.090	1.937	1.935	26.8	3.01	115.0	112.5
60	Stanag	0.090	1.928	1.926	27.1	2.99	115.4	113.0
61	Stanag	4.167	2.006	1.926	19.3	3.46	129.0	120.5
62	Stanag	4.232	1.999	1.918	19.5	3.27	121.0	117.0
63	Stanag	8.648	2.088	1.922	10.9	4.37	136.0	134.5
64	Stanag	8.719	2.097	1.929	10.4	4.38	139.0	131.5
65	Stanag	11.11	2.148	1.933	5.57	4.69	158.0	146.5
66	Stanag	11.14	2.133	1.919	6.20	4.88	148.0	136.0
67	Stanag	14.15	2.198	1.926	0.09	4.97	169.0	152.5
68	Stanag	14.15	2.201	1.928	0.00	5.57	164.5	153.5
69	Clay	26.50	1.929	1.525	0.00	7.82*	97.0	95.0
70	Clay	26.90	1.925	1.517	0.00	7.79*	100.0	98.0
71	Clay	27.30	1.862	1.463	0.00	7.69*	101.0	97.0
72	Minepot	-	-	-	-	2.63	141.8	138.5
73	Minepot	-	-	-	-	2.65	145.0	139.5
74	Minepot	-	-	-	-	2.60	144.0	140.5

This is shown in Fig. 7b where the points at zero air voids account for a 36% variation in delivered impulse. It is appreciated that three very different soil types are represented: LB a cohesionless uniform sand, Stanag a well-graded cohesionless sandy-gravel, and Clay a cohesive fine-grained silty clay. These differing soils have markedly different constitutive properties, which when combined with a numerical model able to incorporate them can lead to excellent agreement between numerical and physical modelling [12, 10].

As a primary single predictor of impulse however, moisture content has been shown to be more highly correlated, indicating its relevance for inclusion in future simplified models to predict loading. For completion, the correlation of impulse with bulk density is also plotted in Fig. 7c. This shows a moderate positive correlation ($r = 0.47$). Bulk density has had success as the sole predictor of impulse in empirical models for mine blast [11], but like air voids has difficulty in differentiating between soil types at full saturation.

Table 4: Correlation between geotechnical parameters and Impulse

	w	ρ	A_v	I
w	1.0000	0.4749	−0.7571	0.9356
ρ	0.4749	1.0000	−0.0937*	0.4710
A_v	−0.7571	−0.0937*	1.0000	−0.7978
I	0.9356	0.4710	−0.7978	1.0000

*Low statistical significance

Table 4 also shows the correlation between geotechnical parameters such as density and moisture content. Due to the wide variety of soils utilised, a high moisture content does not necessarily equal a high density. The correlation is almost identical to that between density and impulse showing that for a single soil type where density increases monotonically with moisture content, bulk density would be an excellent indicator of impulsive output.

In the sub-test series a, b & c, the bulk density, dry density, and air voids were kept constant respectively. The data from these test series at low moisture contents have been replotted in Fig. 8.

4.1.2. Series a

In Fig. 8a, where bulk density was held constant, the LBa data show a moderate positive trend ($r = 0.42$), however this does include the outlier at 2.5% moisture content ($I = 3.14$ kNs). With this data point removed the correlation increases dramatically to $r = 0.73$ for which the trend line is plotted. This indicates that with no change of the overall mass in the system, as the moisture content increases the impulse delivered to a target will also increase (as the moisture content increases, the dry density of the soil decreases).

These findings support general observations that moisture content plays a more important role in governing the output from a buried charge than its density alone would suggest. This trend is only true for LB due to the difficulties in preparing the LBF as noted previously [14], due to it having an increased variation in particle size compared to LB. There does exist a weak negative correlation ($r = -0.34$) in the LBF data, but this is not statistically significant ($p = 0.28$).

Due to the nature of test series a, there are only a limited number of low moisture contents which can be used before the minimum dry density of the soil was reached.

4.1.3. Series b

In test series b (Fig. 8b) the dry density of the soils were held constant while the moisture content and hence bulk density was increased. All soils in this series show a positive correlation between moisture content and impulse, ranging from $r = 0.46$ in the LBF to $r = 0.88$ and $r = 0.84$ for the 2LB and LB respectively. It should be noted that these are the trends for the low moisture content data only.

In test series b the moisture content can be increased to full saturation, at which point the individual soil correlations are within 0.02 of the overall dataset correlation of $r = 0.97$ in Fig. 7a. These data support previous findings where more uniformly-graded soils (LB and 2LB) produced more repeatable soil beds and hence a higher correlation [14].

4.1.4. Series c

In the final test series, the air voids present in the soil were kept constant, leading to a rapid decrease in dry density as moisture content was increased. The results presented in Fig. 8c show a positive correlation ($r = 0.62$) which, when compared to the strong correlation between moisture content and impulse ($r = 0.94$), emphasizes the importance of using moisture content as a primary metric over air voids.

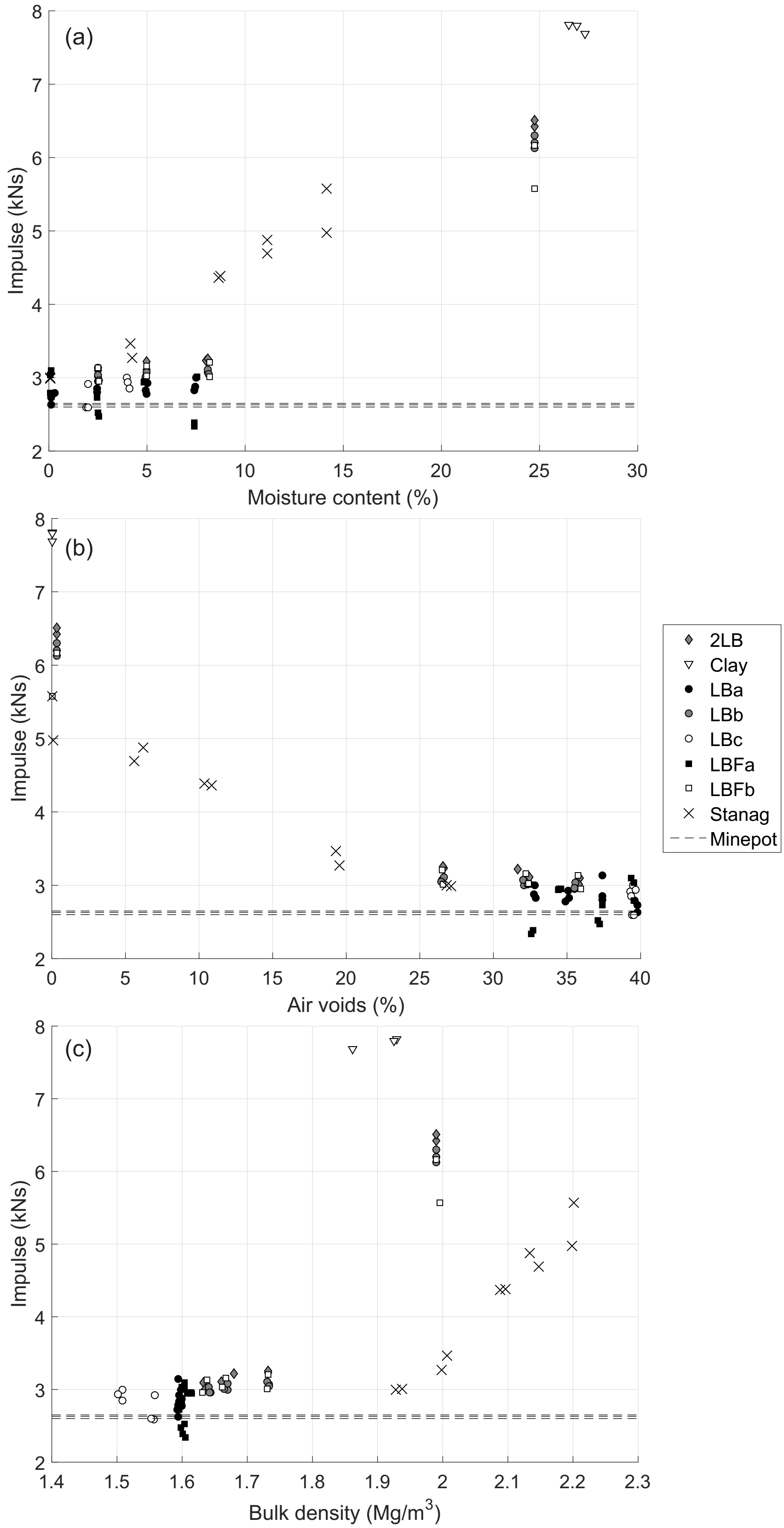

Figure 7: Impulse versus (a) moisture content, (b) air voids and (c) bulk density

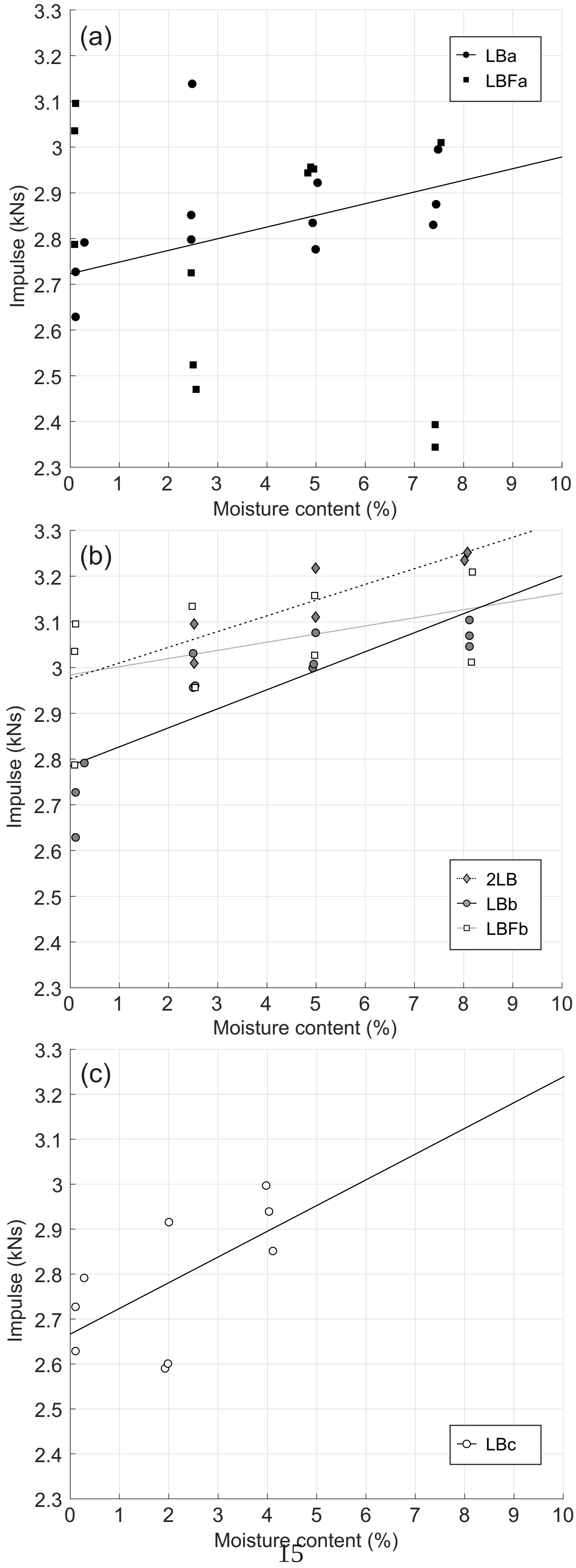

Figure 8: Impulse at low moisture contents. Test series: (a) constant bulk density (b) constant dry density, and (c) constant air voids

4.2. *Scaling particle size distributions*

To directly assess the effect of possible scaling issues on the grain size of the soil when moving between full and half-scale testing, tests were conducted with two variations of LB. The standard LB used has a particle size range between 0.6–1.18 mm (midpoint particle size, D_{50} = 0.87 mm), the second variant, 2LB has particles twice as large (range = 1.18–2.8 mm, D_{50} = 1.76 mm). This means that 2LB at the current scale is geometrically identical to LB at full-scale. Comparison of the results from the two soils can therefore be used to determine whether scaling the particle size is also required when moving to half-scale testing. The impulse results in Fig. 7a and highlighted further in Fig. 8b show no clear systematic difference between the LB(b) and 2LB results (r = 0.84 and r = 0.88) indicating that scaling of the grain size at half-scale testing is not required. It should be noted that the difference between the trend lines in Fig. 8b is caused by the exclusion of the full saturation data. The average difference between the trendlines plotted through the entire LBb and 2LB dataset is 2.5%, which is within the experimental error for both soils reported in [14]. Any further scaling down of the test arrangement would require further validation to check that the soil is still indicative of its full-scale equivalent.

4.3. *Factors affecting plate deflection*

For each test the peak and residual deflections were recorded. Fig. 9 show the peak deflection plotted against moisture content, air voids and bulk density. Interestingly the primary predictor of impulse is not the same as that for plate deflection. Fig. 9a shows the correlation of peak deflection versus moisture content. Whilst there is a moderate positive correlation (r = 0.47), soil type plays a more important role, highlighted by the results at full saturation where there is a 50% spread of deflection between the Stanag, LB and Clay soils. As was discussed previously, the use of the Minepot not only lowers impulse delivered but also the peak target deflections when compared with the fully-saturated Stanag. Air voids are shown to be a more correlated predictor of plate deformation as shown in Fig. 9b (r = −0.76). This value does include the cohesive soils which no not conform to the same trends, indicating that the mode of delivery of the impulse may well be different, as explored in the next section. In the final plot

Fig. 9c, peak deflection is plotted against bulk density. The overall correlation is stronger than with moisture content ($r = 0.56$). It is worth noting that this overall trend with bulk density incorporates all soils rather than being an excellent fit for cohesionless soils only.

Thus far each of the geotechnical factors have been plotted against peak deflection. Rather than also plotting all the data against residual deflection, peak deflection has been plotted against residual deflection in Fig. 10. With an R^2 value of 0.98, the deflections are almost perfectly proportional, with peak deflection being 7.5% higher than the corresponding residual deflection (post elastic strain recovery), as would be expected. Therefore, the trends for peak deflection outlined previously are equally applicable for residual deflection in this experimental configuration.

4.4. Impulse and deflection interactions

To further interrogate the dataset, peak deflection was plotted against impulse for all the tests conducted, Fig.11. For all the cohesionless soil tests the data lie in a band where peak deflection is approximately proportional to the impulse delivered. It is postulated that the factor driving deflection is the degree of focus of the generated blast. The best example of this focussing effect is the Minepot, which is able to drive a high deflection despite delivering a relatively low impulse. Alternatively, the Clay data show very low deflections despite having the highest impulse, indicating that the loading is delivered in a less focussed, more spatially uniform way.

5. Development of a predictive model for impulse

Predicting the impulsive output from buried charges is highly dependent on the physical test arrangement used. Whilst the effects of a specific combination of soil type, charge size, and burial geometry can be determined through experimentation or numerical analysis, the aim of this paper is to develop a simplified predictive model that indicates how the geotechnical conditions can effect the impulse generated by a buried charge in a *relative* way. For impulse, moisture content has been shown to be the driving geotechnical condition, however bulk density also been shown to have a secondary effect in mediating impulse. In this article an impulse modification factor (I_{mod}) is developed based on the combined effects of moisture content and

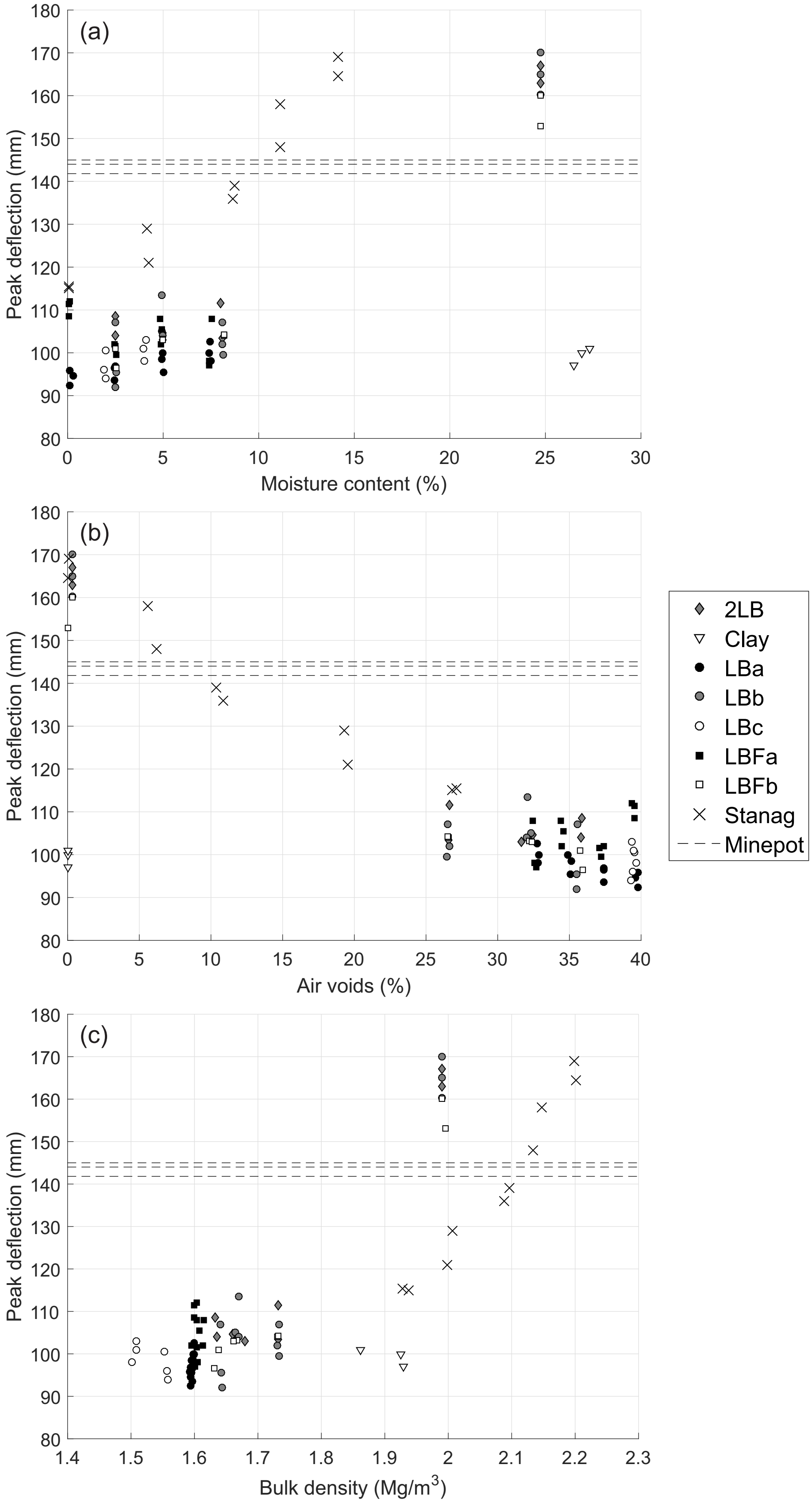

Figure 9: Peak plate deflection versus (a) moisture content, (b) air voids and (c) bulk density

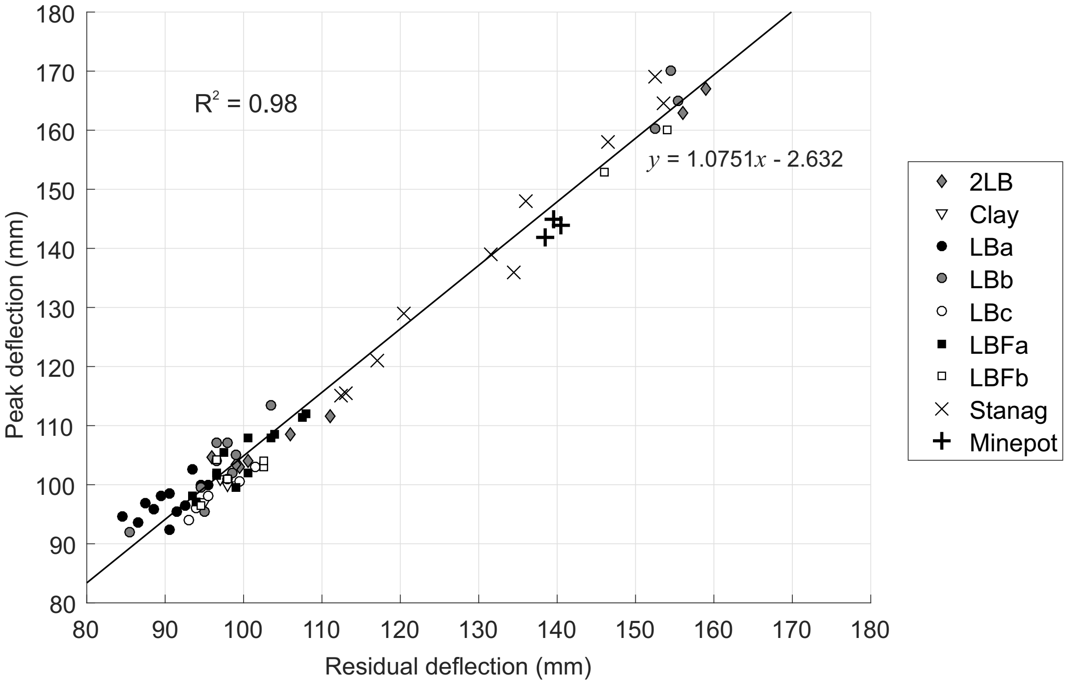

Figure 10: Peak versus residual plate deflection

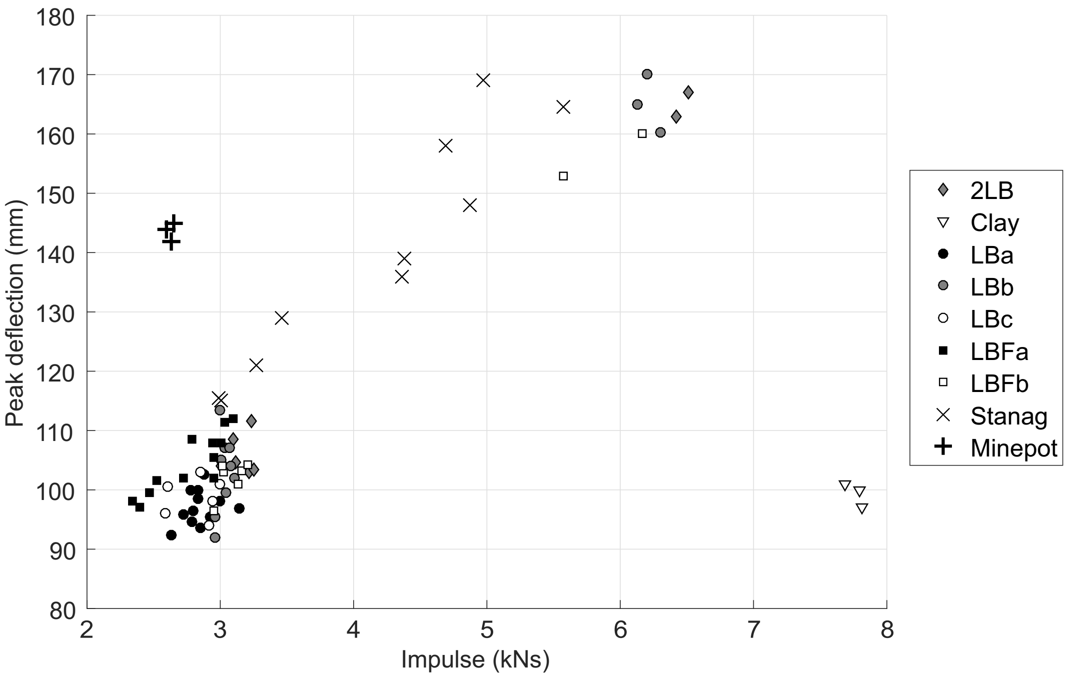

Figure 11: Peak plate deflection versus impulse

bulk density, which, when used to multiply the known impulse from a reference condition, can give a first-order estimate of the impulse delivered to a target situated above the soil bed.

The reference condition in the proposed model ($I_{mod} = 1$) is that of a dry uniform sand (LB) with a bulk density of 1.6 Mg/m^3, representing the lowest mass and moisture content combination likely to be present in the natural environment. The impulse from each test was divided by the average reference condition impulse to give a normalised value. A multiple linear regression analysis was then conducted to assess the individual contributions of both geotechnical parameters on impulse. The impulse modification factor, I_{mod} (unitless), is given in Equation 1, where w is moisture content in percent and ρ is bulk density in Mg/m^3. The results of this equation are shown in Fig. 12a with the higher the moisture content and bulk density the greater the factor on the reference impulse.

$$I_{mod} = 0.89935 - 0.095907w + 0.033118\rho + 0.077821w\rho \tag{1}$$

As the predictive method is intended to be first-order accurate, it is important to consider the potential error in the calculated impulse. The model error is plotted against both bulk density and moisture content in Figs. 12b and c respectively to identify any areas where the model is less accurate. The relative standard deviation of the model predictions is 0.0953, with 1σ and 2σ bounds (representing the 68 and 95% confidence intervals) also shown in Figs. 12b and c. Hence as there is a 95% probability that the calculated impulse is within ±20% of the actual value. The mean absolute model error across the whole data series (experimental impulse/prediction) is 7.3%.

When considering the accuracy of the model across the entire data series, it is worth noting the following:

- The influence of moisture content on impulse becomes less significant for moisture contents below 8%. Whilst Figure 8b shows that the impulse delivered to a target will increase with increasing moisture content when the bulk density of the soil is kept constant, the model will over-predict this effect. This can be seen in Fig. 12c where the model gives an impulse value that is consistently lower than the experiments at 0% moisture content and consistently higher than the experiments at 8% moisture content.
- Bulk density effects are less well accounted for at bulk densities below 1.8 Mg/m^3. This is due to the minimal influence of bulk density on impulse at these values (see Fig. 7),

particularly at low moisture contents. This produces a region of near-unity modification factors towards the bottom-left of Fig. 12a. Despite this, the model is still accurate to ±20% in this range.

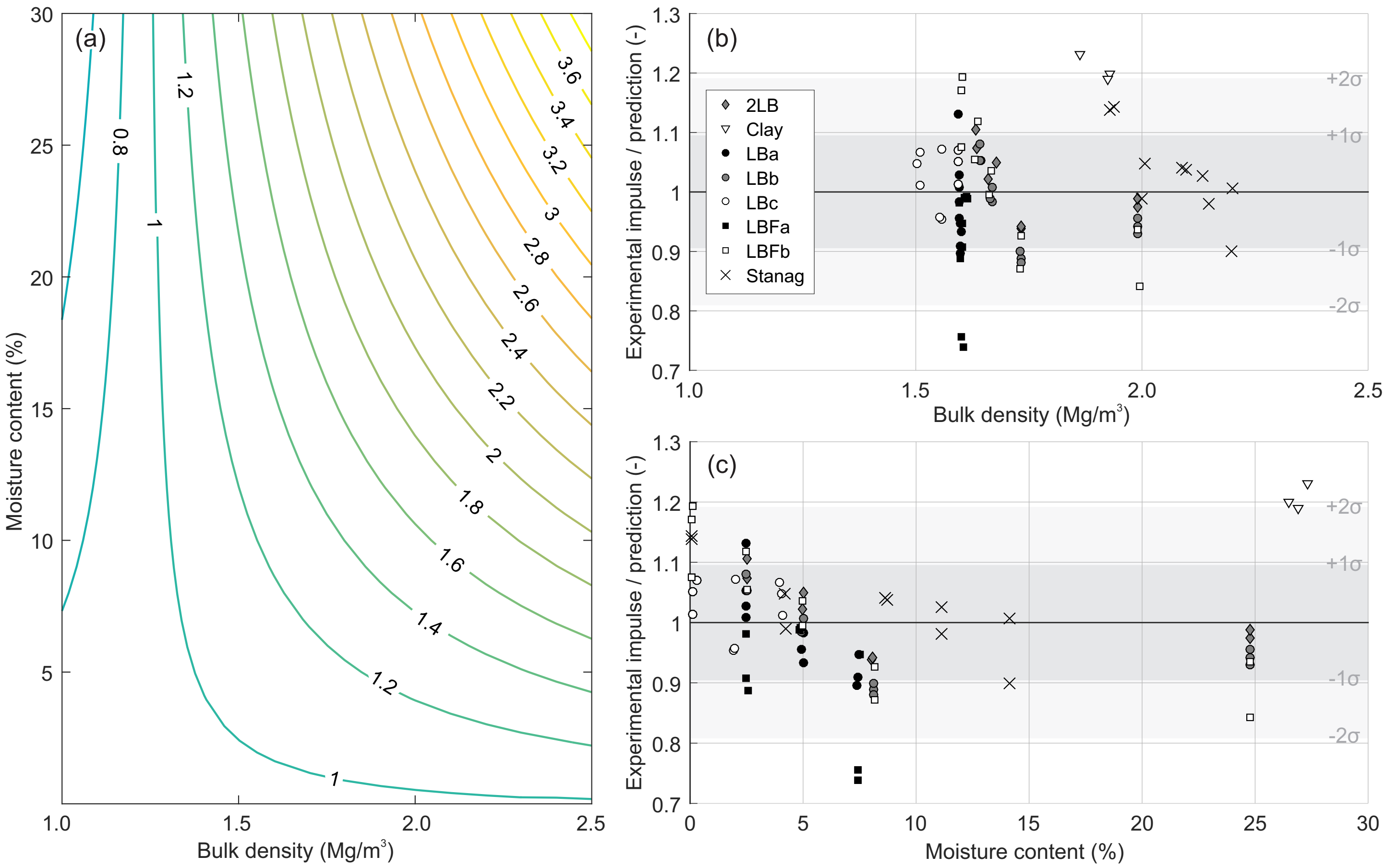

Figure 12: Output from predicted model (a) lookup table for modification factor (I_{mod}) to account for geotechnical parameters. Experimental factor divided by the predicted factor plotted against (b) bulk density (c) moisture content

5.1. Worked example 1: geotechnical variance

The predictive model requires a reference condition to which the calculated modification factor is applied. The reference condition consists of a specific bulk density and moisture content at which the impulsive output from a physical test is known. This allows any changes in geometry (from the test conditions presented in this paper) to be appropriately incorporated.

The reference condition used in this example is that of dry LB at a bulk density of $\approx$ 1.6 Mg/m^3. From Table 3 it is known that impulse delivered from a 625 g charge buried at 50 mm will be $\approx$ 2.7 kNs. From the reference condition it is possible using the modification factors in

Fig. 12a to assess the range of impulses achievable with variations in moisture content (and bulk density as the two are intrinsically linked). From Fig. 12a, dry soil ($w = 0\%$, $\rho = 1.6$ Mg/m^3) has a corresponding modification factor of ≈ 1.0.

By using Fig. 12a the modification factor can be assessed for any change in geotechnical conditions. For example at full saturation, the moisture content and density both change, in this case $w = 25\%$ and $\rho = 2$ Mg/m^3, giving a modification factor of ≈ 2.4 (2.459 using Eq. 1). By multiplying the measured reference condition impulse by the modification factors the range of impulses can be generated. This leads to a range in impulse from 2.7 kNs for a dry soil in the reference condition to 6.48 kNs (6.64 kNs using Eq. 1) for a saturated soil, which when compared with the experimentally measured results (2.63–6.03 kNs) is within the error of the model and provides an indicative first-order estimate.

5.2. *Worked example 2: impact on numerical models*

The assessment of impulse variation is also applicable to numerical modelling. One of the most easily accessible models for the prediction of mine loading is the empirical method outlined by Tremblay [20], based on the original work by Westine et al. [11]. This model includes bulk density as an input parameter, but does not explicitly include moisture content effects. The predictive model in this paper can therefore be utilised to modify the Tremblay-calculated impulse to account for moisture content effects.

The Tremblay model gives the total impulse acting on a plate, I, as

$$I = 0.1352\left(1 + \frac{7\delta}{9z}\right)\sqrt{\frac{\rho E}{z}}\int_{x_0}^{x_1}\int_{y_0}^{y_1}\left(\frac{\tanh(0.9589\zeta d)}{\zeta d}\right)^{3.25} \mathrm{d}y\mathrm{d}x \tag{2}$$

where the symbols used in Equation 2 are given in Table 5 and have been evaluated for the experimental arrangement in the current article. This equation was solved through numerical integration using MatLab. The value of $E/A\rho c^2 z = 3.3953$ is below the lower limit of 6.35, and hence the results are extrapolated slightly beyond the range suggested by Tremblay.

In Fig. 13, Equation 1 is plotted for moisture contents between 0 and 20%, at 5% increments, and for bulk densities between 1.4 and 2.3 Mg/m^3. The output from the Tremblay model is plotted as the dashed line, where the results have been normalised against the Tremlbay-predicted impulse at a reference condition of $\rho = 1.6$ Mg/m^3. As shown in Fig. 13, at a bulk density of 2.1 Mg/m^3 Tremblay model result lies between the 0 and 5% moisture content lines.

Table 5: Input parameters for the Tremblay model

Parameter	Symbol	Value
Burial depth (from charge centre)	δ	$0.038/2 + 0.05 = 0.069$ m
Standoff (from charge centre)	z	$\delta + 0.1375 = 0.2065$ m
Soil density	ρ	1600 kg/m^3
Explosive mass	W	0.625 kg
Energy release in explosive charge	E	W $\times$ 6.7E6 = 4187500 J
Cross-sectional area of mine (in plan)	A	$\pi \times (0.115/2)^2 = 0.104$ m^2
Seismic P-wave velocity	c	500 ms^{-1}
Plate dimensions	x_0	-0.3375 m
	x_1	$+0.3375$ m
	y_0	-0.3375 m
	y_1	$+0.3375$ m
Lateral distance to centre of mine	d	$\sqrt{x^2 + y^2}$
Tremlay parameter	ζ	$\dfrac{\delta}{z^{5/4} A^{3/8} \tanh\left(\left(2.2\dfrac{\delta}{z}\right)^{3/2}\right)} = 0.0499$ m^{-1}

The Tremblay model does not explicitly account for moisture content effects. The modification factor, I_{mod}, determined from Equation 1, can be applied to the Tremblay model prediction to account for this. In the case of a soil with a moisture content of 10% and bulk density of 2.1 Mg/m^3, using the impulse modification factor derived in this article alone would give a factor of 1.56 to apply to the reference condition of the impulse from dry soil at a bulk density of 1.6 Mg/m^3. However, as the Tremblay model already includes allowances for bulk density effects, the modification factor of 1.56 cannot be directly applied to the results. The Tremblay model predicts a normalised impulse of 1.15 when accounting for bulk density effects alone at $\rho = 2.1$ Mg/m^3. The correct modification factor to apply to the Tremblay reference condition would therefore be the modification factor calculated from the predictive method in this article at 10% moisture content, divided by the dry Tremblay normalised impulse, i.e. $1.56/1.15 = 1.36$. This modification factor can then be applied directly to the results from the Tremblay model to account for the combined effects of bulk density and moisture content. Clearly this method relies on an accurate underlying model, however its use as an indicative first-order estimate for the variation generated by changing geotechnical conditions is valid regardless of the reference condition.

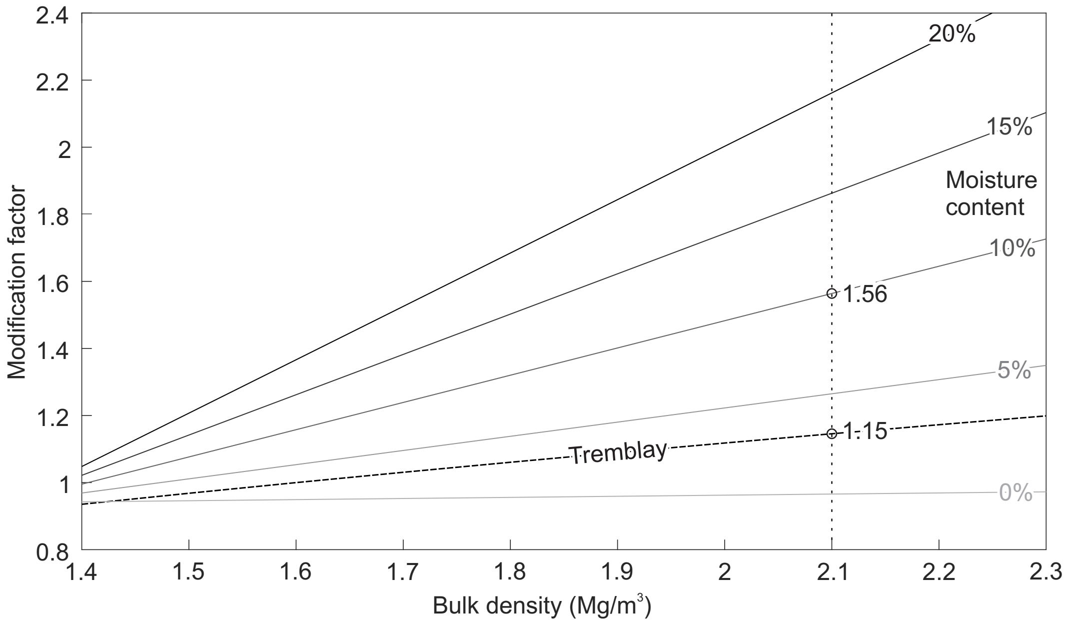

Figure 13: Predicting the possible influence of moisture content on the impulse generated by the Tremblay model

6. Conclusions

It has been shown that moisture content is the primary geotechnical condition which governs the impulsive output from a shallow buried charge with a positive correlation, *r*, of 0.9356. By moving from a dry to a saturated sand the impulsive output can be more than doubled.

Whilst air voids are also a good indicator of impulse output their inability to distinguish between soils at full saturation is problematic for use in any predictive model. This was confirmed by conducting separate test series at low moisture contents specifically looking at keeping the air voids, dry, and bulk densities constant and comparing the impulses. This study showed that for soils which have identical air void ratios, the effect of increasing moisture content (whilst decreasing mass) still has the effect of increasing impulse.

As many soils were utilised in the work the effect of scaling particle sizes by a factor of 50% was also investigated by testing with LB and 2LB soils. This showed no noticeable effect on the output from tests in both soils for both deflection and impulse measurements, validating the use of ‘full scale’ soils in the current testing and removing the need to scale down the soil particle distributions. However, further work would be required to validate this approach below the half-scale testing current conducted.

The primary geotechnical condition which governs plate deflections was found to be air voids. It is hypothesised that this is due to the confinement given to the detonation products by the soil. For cohesionless soils this means that the less compressible the soil (the lower the air voids) the more confinement given to the detonation products, and hence the loading is more localised and the deflections larger. This is only true however for cohesionless soils. In the case of cohesive soils (clay) the deflections were 40% lower due to a lower degree of focusing of the loading. The Minepot results conversely gave a much higher deflection than the impulse measured during the testing would suggest. For nominally identical test setups, a uniform blast load will have a higher impulse:deflection ratio whereas a focussed load will deliver a lower impulse:deflection ratio. The exact nature of this loading is currently being investigated further by the authors [21, 22].

A first-order predictive model for the impulse from a buried charge has been proposed based on the results presented herein, which allows researchers to gain an estimate of the effect that changing the bulk density and moisture content of the soil surrounding a buried charge has on the impulse output. It is hope that this will provide a simple assessment tool for numerical model error analyses and for fast running engineering models.

Acknowledgements

The authors wish to thank the Defence Science and Technology Laboratory (DSTLX-1000059883) for funding the published work.

References

[1] A Neuberger, S Peles, and D Rittel. Scaling the response of circular plates subjected to large and close-range spherical explosions. Part II: Buried charges. *International Journal of Impact Engineering*, 34(5):874–882, 2007.

[2] Pickering EG, Chung Kim Yuen S, Nurick, GN, Haw P. The response of quadrangular plates to buried charges. *Int J of Impact Eng*, 49:103–114, 2012.

[3] Shaowen Xu, Xiaomin Deng, Vikrant Tiwari, Michael a. Sutton, William L. Fourney, and Damien Bretall. An inverse approach for pressure load identification. *International Journal of Impact Engineering*, 37(7):865–877, 2010.

[4] Bergeron DM, Trembley JE. Canadian research to characterize mine blast output. *16th Int Sym on the Military Aspects of Blast and Shock, Oxford, UK*, 2000.

[5] Hlady SL. Effect of soil parameters on landmine blast. *18th Int Sym on the Military Aspects of Blast and Shock, Bad Reichenhall, Germany*, 2004.

[6] Fourney WL, Leiste U, Bonenberger R, Goodings DJ. Mechanism of loading on plates due to explosive detonation. *Int J on Blasting and Fragmentation*, 9(4):205–217, 2005.

[7] Anderson CE, Behner T, Weiss CE. Mine blast loading experiments. *Int J of Impact Eng*, 38(8-9):697–706, 2011.

[8] Fox DM, Huang X, Jung D, Fourney WL, Leiste U, Lee JS. The response of small scale rigid targets to shallow buried explosive detonations. *Int J of Impact Eng*, 38(11):882–891, 2011.

[9] Ehrgott JQ, Rhett RG, Akers SA, Rickman DD. Design and fabrication of an impulse measurement device to quantify the blast environment from a near-surface detonation in soil. *Experimental Techniques*, 35(3):51–62, 2011.

[10] Fox DM, Akers SA, Leiste UH, Fourney WL, Windham JE, Lee JS, Ehrgott JQ, Taylor LC. The effects of air filled voids and water content on the momentum transferred from a shallow buried explosive to a rigid target. *Intl J of Impact Eng*, 69(0):182–193, 2014.

[11] Westine PS, Morris BL, Cox PA, Polch E. Development of computer program for floor plate response from landmine explosions. *Contract Report No. 1345, for US Army TACOM Research and Development Center*, 1985.

[12] Grujicic M, Pandurangan B, Cheeseman BA. The effect of degree of saturation of sand on detonation phenomena associated with shallow-buried and ground-laid mines. *Shock and Vibration*, 13(1):41–61, 2006.

[13] Deshpande VS, McMeeking RM, Wadley HNG, Evans AG. Constitutive model for predicting dynamic interactions between soil ejecta and structural panels. *Journal of the Mechanics and Physics of Solids*, 57(8):1139–1164, 2009.

[14] Clarke SD, Fay SD, Warren JA, Tyas A, Rigby SE, Reay JJ, Livesey R, Elgy I. Geotechnical causes for variations in output measured from shallow buried charges. *Intl J of Impact Eng*, 86(0):274–283, 2015.

[15] NATO. Procedures for evaluating the protection level of armoured vehicles - mine threat. *Allied Eng. Publication (AEP) 55*, Vol.2, Edition C, Version 1, May, 2014.

[16] NATO. Protection levels for occupants of armoured vehicles. *STANAG 4569*, Edition 3, 23 May, 2014.

[17] S.D. Fay, S.E. Rigby, A. Tyas, S.D. Clarke, J.J. Reay, J.a. Warren, and R. Brown. Displacement timer pins: An experimental method for measuring the dynamic deformation of explosively loaded plates. *International*

Journal of Impact Engineering, 86:124–130, 2015.

[18] DSTL. UK ministry of defence technical authority instructions for testing the protection level of vehicles against buried blast mines. *DSTL (draft)*, 2012.

[19] X. Zhao, V. Tiwari, M. A. Sutton, X. Deng, W. L. Fourney, and U. Leiste. Scaling of the deformation histories for clamped circular plates subjected to blast loading by buried charges. *International Journal of Impact Engineering*, 54:31–50, 2013.

[20] Tremblay JE. Impulse on blast deflectors from a landmine explosion. *DREV Technical memorandum, DREV-TM-9814*, 1998.

[21] Clarke SD, Fay SD, Warren JA, Tyas A, Rigby SE, Elgy I. A large scale experimental approach to the measurement of spatially and temporally localised loading from the detonation of shallow-buried explosives. *Measurement Science and Technology*, 26:015001, 2015.

[22] S.E. Rigby, S.D. Fay, S.D. Clarke, A. Tyas, J.J. Reay, J.A. Warren, M. Gant, and I. Elgy. Measuring spatial pressure distribution from explosives buried in dry leighton buzzard sand. *International Journal of Impact Engineering*, 96:89 – 104, 2016.